CHINESE OPTICS LETTERS

Vol. 20, No. 2 | February 2022

High-color-purity, high-brightness and angle-insensitive red structural color

Jintong Liu (刘晋彤), Kun Feng (冯 坤), Yusi Wang (王雨思), Qingyuan Li (李青原), Nan Chen (陈 楠), and Yikun Bu (卜轶坤)*

School of Electronic Science and Engineering (National Model Microelectronics College), Xiamen University, Xiamen 361005, China

*Corresponding author: buyikun0522@xmu.edu.cn

Received July 15, 2021 | Accepted August 17, 2021 | Posted Online October 8, 2021

We propose a simple five-layer structure for creating red structural color, which has high color purity and high brightness. The design is based on the superposition of a silver substrate and multilayer silicon material. Absorption at the shorter wavelengths of the structure is effectively guaranteed, and reflection at the longer wavelengths is well enhanced. The red structural color has a peak reflectivity of 91% and a colorimetric purity of 0.9. Moreover, the designed structure displays angle-invariant performance up to 60°. This kind of structure scheme is environmentally friendly with low fabrication cost, and it can play an important role in a variety of fields, such as color displays and image sensors.

Keywords: structural colors; absorption; thin films.
DOI: 10.3788/COL202220.021601

1. Introduction

Structural colors can achieve optical effects, such as interference, diffraction, and scattering of light by using the fine micro-nanostructure on the surface of organisms, showing gorgeous colors[1–3]. Because of its advantages of non-fading, low pollution, and iridescent effect, structural colors have broad application prospects in display, decoration, anti-counterfeiting, and other fields, such as making cosmetics and military paint with anti-counterfeiting colors[4–6]. Among them, structural colors are widely used by thin films, owing to their simple structure, controllable color, and good reproducibility. Structural colors have important applications in the fields of color displays, light-emitting diodes, and image sensors[7–10]. Traditional filters based on organic dyes or chemical colorants are susceptible to environmental factors, such as temperature, moisture, and light, thus reducing the service life of filters[11–13]. To avoid these difficulties, structural colors have been proposed as alternatives.

The basic working principle of color design is the thin-film interference effect of light. When the incident angle of light changes, the spectral properties of the thin films will also change, resulting in different colors[14–17]. Especially, in some fields, such as display, structural colors with certain angle tolerance are often needed. We hope that the spectral reflection characteristics of the thin films will not change and deteriorate with the change of incident angle[18–20]. Therefore, the angle-insensitive thin films are an important development direction for structural colors[21–23]. Among various current color filter schemes, the realization of red color has always been a difficult problem. There is a lot of research on how to achieve high-purity and high-brightness red color. Kats *et al.* proposed a structure of plating ultra-thin absorption layers on a metal substrate. Gold is used as the substrate, and germanium is plated on it with a 10 nm thickness[24]. The structure can selectively absorb various frequency ranges of incident light and has low sensitivity to incident angles. The combination of metal and thin absorbing layer can be used to achieve red color. However, the short-wavelength reflection of this structure is high (greater than 20%), resulting in low color purity. Chen *et al.* designed a color filter with a Fabry–Perot (F-P) structure, in which copper is sandwiched between two layers of amorphous silicon (a-Si), and the peak reflection can reach about 80% by using the higher-order F-P cavity resonance[25]. The F-P structure is based on the principle of F-P resonance. This structure can compress the reflection peak, but its absorption bandwidth in the visible region is narrow and difficult to adjust. The short-wavelength absorption capacity of the structure is limited, so the color purity is still not high enough. Lee *et al.* proposed a red structural color based on silicon materials (a-Si and silicon nitride), which significantly suppresses short-wavelength reflection and reduces the reflection in the 400–600 nm wavelength range to less than 5%[26]. This kind of silicon structure has great absorption in the entire visible light range. Although the short-wavelength reflection is greatly suppressed, the long-wavelength reflection has difficulty reaching a high level due to its absorption character, resulting in low color brightness. Therefore, achieving high-color-purity, high-brightness, and angle-insensitive red structural color is still a challenge.

In this study, we demonstrate a silver (Ag)-based simple five-layer structure in order to compress short-wave sub-peak and reduce long-wavelength absorption. Using the absorption characteristics of a-Si, silicon monoxide (SiO) and other materials realize the selective absorption of the spectrum, so that the absorption of the thin films is high at the shorter wavelengths but low at the longer wavelengths. The absorption of the proposed structure is more than 96% below 550 nm, and it gradually decreases to 8% in the 650–750 nm region. Meanwhile, we use antireflection (AR) layers to further suppress the remaining sideband reflection. We designed and produced a five-layer red structural color. This structure is based on metallic Ag, which has high reflection, low short-wavelength reflection, and high long-wavelength reflection. The average residual reflection of this structure in the 400–550 nm wavelength range is 2.35%, the average reflection of red range (650–750 nm) is 78.65%, and the peak reflection is 91%. The colorimetric purity of the red color obtained through experiment is 0.9. The thin films are simple in structure, and finally realize red structural color with low angle sensitivity, high color purity, and high brightness. This one-dimensional lamellar thin-film structure is easy to mass produce through the conventional physical vapor deposition (PVD) process. It has a wide range of applications in optical display, optical anti-counterfeit, decoration, stealth, and other fields.

2. Structure and Design

The focus of our design is to create an angle-insensitive red color with higher purity and higher brightness. At visible wavelengths, red belongs to the long wave, and the color in the region of the short wavelength will affect the purity of red. To solve this problem, we increase short-wavelength absorption and use AR layers. The designed five-layer structure, which can produce angle-insensitive red color in the range of 0° to 60°, is shown in Fig. 1(a). The structure has a high color purity, which is achieved by using the overlapping of high and low refractive index materials to produce steep reflection in the long-wave range and suppress sideband reflection.

Figure 1(a) shows a schematic diagram of the proposed structure, which consists of four materials with different refractive indices alternately stacked. The bottom layer is Ag with the thickness of 100 nm. In our study, Ag is selected as the material of the bottom metal because it has the lowest material absorption loss and the highest reflectivity in all visible wavelength ranges of all metals. In the 400–800 nm band, the refractive index of Ag varies from 0.05 to 0.09, and the extinction coefficient varies from 1.93 to 5.45. The thickness of the SiO_2 layer above the Ag is 82 nm, and the thickness of a-Si is 56 nm. Under different experimental conditions, the optical constants of a-Si are quite different. Figure 1(b) shows the optical constants of a-Si

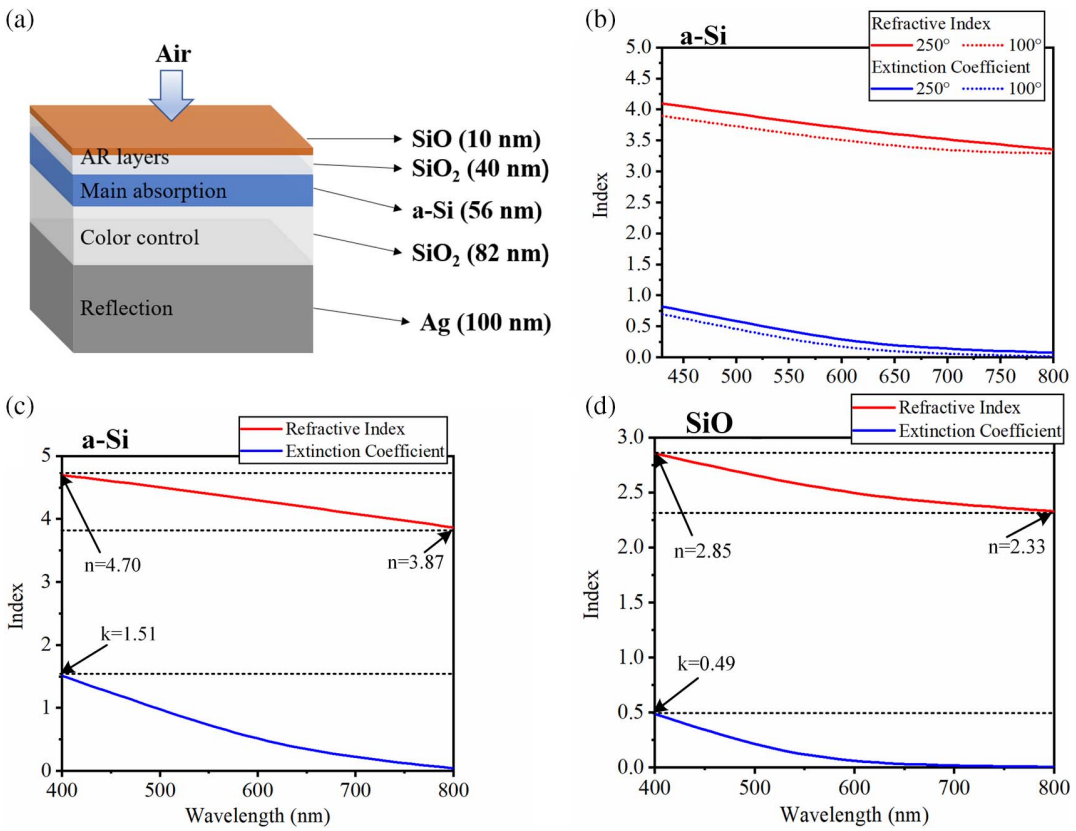

Fig. 1. (a) Schematic view of the proposed structure. (b) Optical constants of a-Si (180 nm) under different experimental conditions. (c) Optical constants of a-Si in the design. (d) Optical constants of SiO.

prepared under different conditions. In this experiment, the refractive index of a-Si in the wavelength range of 400 to 800 nm is 3.87–4.70 using electron beam evaporation, as shown in Fig. 1(c). The a-Si and SiO are used as high refractive index materials, while SiO_2 is used as a low refractive index material. During the experiment, SiO_x was prepared by controlling the temperature and oxygenation, and the optical constants of the obtained SiO are shown in Fig. 1(d). During the deposition of the Ag layer, the increase of substrate temperature will lead to crystallization of the underlying Ag layer, resulting in the increase of surface roughness of the layer. The roughness seriously affects the performance of this structure. Firstly, we deposit the bottom Ag layer at room temperature. Then, we heat up the device to 150°C and finally deposit other materials in sequence. The reason why other materials are deposited at 150°C is that the a-Si prepared at this temperature can obtain good absorption performance to meet the needs of our design.

For the color design in the spectrum, it is necessary to compress the reflection bandwidth and eliminate the reflection subpeak for improving color purity. Since a-Si is a kind of material with high refractive index, the reflective index difference between a-Si and air is large, which will lead to a considerable amount of reflection in the 400–600 nm wavelength range. So, it affects the purity of the red color. The top two layers of

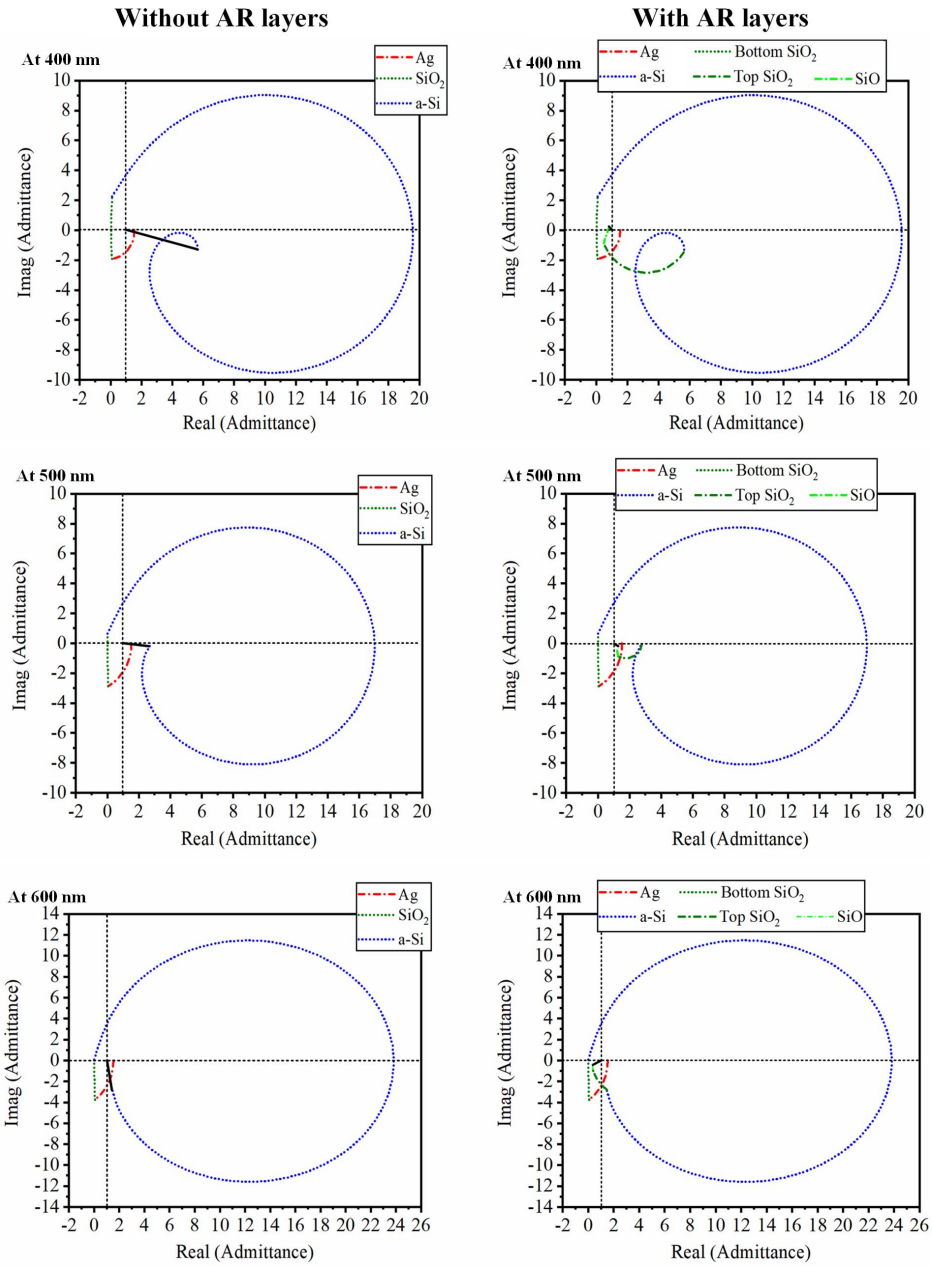

Fig. 2. Optical admittance diagrams of the structure without and with the AR layers at 400 nm (first row), 500 nm (second row), and 600 nm (third row). The intersection of the two black dashed lines represents the point (1,0).

the structure, SiO and SiO_2, are used as AR layers to suppress sideband reflection. The suppression of sideband reflection is achieved by admittance matching, and we can investigate the AR layers by using the optical admittance diagram to further verify its effect. Optical admittance is numerically equal to the refractive index of the material. Assume that there is a single-layer film with an admittance of n on a substrate that has an admittance of $\alpha + i\beta$; then,

$$x^2 + y^2 - \frac{\alpha^2 + \beta^2 + n^2}{\alpha} x = -n^2. \tag{1}$$

This is the equation of a circle whose center coordinate is

$$\left(\frac{\alpha^2 + \beta^2 + n^2}{2\alpha}, 0\right) \tag{2}$$

and that passes through the point (α, β). It can be seen that the admittance trajectory of thin films is composed of a series of circles or arcs that meet each other, and each arc corresponds to a different layer. In the case of a transparent medium and perfect conductor, the trajectory of the admittance is a complete circle. But, in the case of an absorbing medium, such as semiconductors and real metals, the extinction coefficient of materials causes the trajectory to spiral. The reflection can be calculated using the following formula:

$$R = \left(\frac{Y_0 - Y_1}{Y_0 + Y_1}\right)\left(\frac{Y_0 - Y_1}{Y_0 + Y_1}\right)^*, \tag{3}$$

where Y_0 and Y_1 are the optical admittances of the starting incident medium and ending point. This formula shows that the reflection can be simply quantified by the distance between the ending admittance point of the structure and the air point (1,0). The closer the ending point is to the air point, the weaker the reflection is. The optical admittance of the structure starts from the point $(n_{sub},0)$ of the glass substrate, and, as the thickness of each layer is increased, the admittance rotates on a circle. In order to reduce the reflection below 600 nm, the admittance of the structure can be exactly matched with the admittance of air. That is, let the ending admittance point of the structure be (1, 0), so zero reflection is achieved. Figure 2 shows the optical admittance diagrams of the structure without and with the AR layers at 400, 500, and 600 nm. Calculated color coordinates of the final admittance (without AR layers) are (5.62, −1.47), (2.77, −0.08), and (1.46, −2.8) for 400, 500, and 600 nm. These points are far away from the air point (1, 0), indicating that the reflection is strong at that wavelength. After adding the AR layers, the calculated ending admittance points are (0.89, 0.32), (1.25, −0.12), and (0.36, −0.19), which are closer to the air point. The results show that the addition of the AR layers greatly suppresses the reflection between 400 and 600 nm.

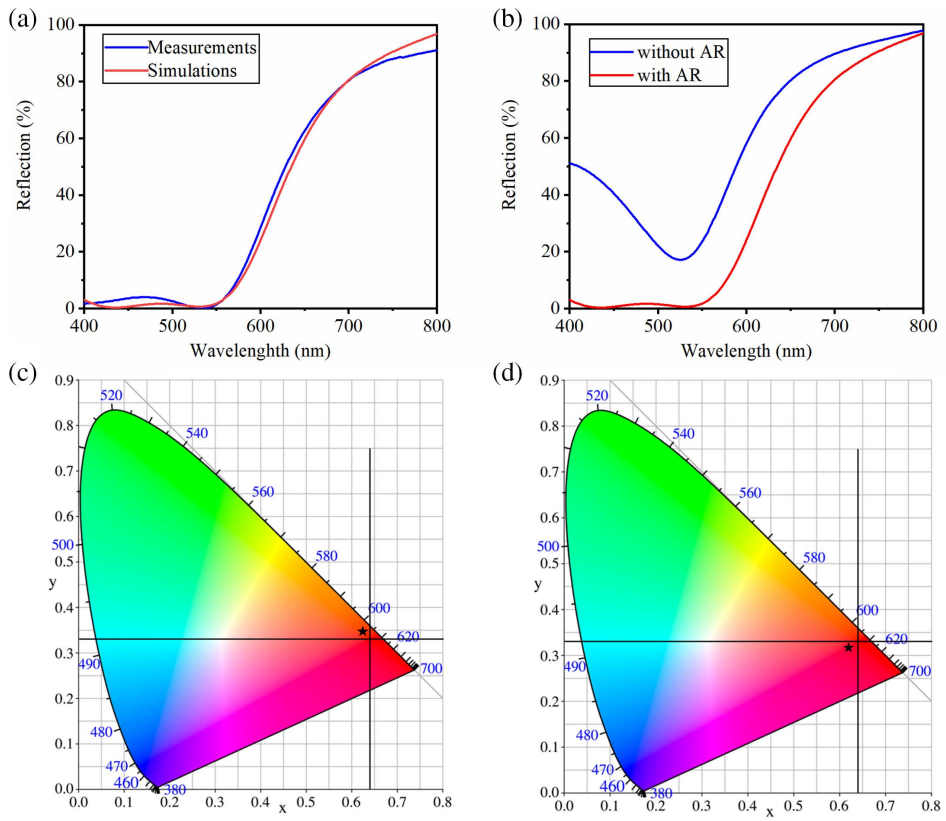

Fig. 3. (a) Calculated (red) and measured (blue) reflection spectra of the proposed device at normal incidence. (b) Calculated spectral reflectance curves with (red line) and without (blue line) the AR layers. (c), (d) Illustration of color coordinates calculated from the reflection spectra in (a) on the CIE 1931 chromaticity diagram.

3. Results and Discussion

The spectral performance of the sample obtained by design and preparation can be calculated intuitively to obtain the color performance. The reflection spectra at normal incidence are obtained with a thin-film measurement instrument (UV-1900I). Figure 3(a) provides the calculated reflection spectra (red) of the designed structure at normal incidence, presenting a good agreement with measured reflection spectra (blue). The reflection spectra obtained with and without AR layers are shown in Fig. 3(b). It can also be seen from the spectrum that the reflection below 600 nm is greatly suppressed, and a peak reflection of 91% is achieved at the longer wavelengths, both of which are conducive to the production of high-purity red color. The color coordinates are evaluated according to the calculated and measured reflections under the standard Illuminant D65 and described on the CIE 1931 chromaticity diagram, as shown in Figs. 3(c) and 3(d). The intersection of two solid black lines in the figure represents the standard red (0.64, 0.33) used in liquid crystal displays (LCDs). As can be seen from the figure, the color coordinates of both the simulated (0.63, 0.34) and the measured (0.62, 0.32) are very close to the standard red used in LCDs. The experimental results show that the red color we designed is of high purity.

The high color purity is the result of the combination of AR layers and the absorption properties of these materials. Traditional single-layer AR coating often uses metal oxide materials, such as TiO_2 and Al_2O_3. The conditions of an ideal single-layer AR coating are as follows: optical thickness of the layer is a quarter of wavelength, and its refractive index is the

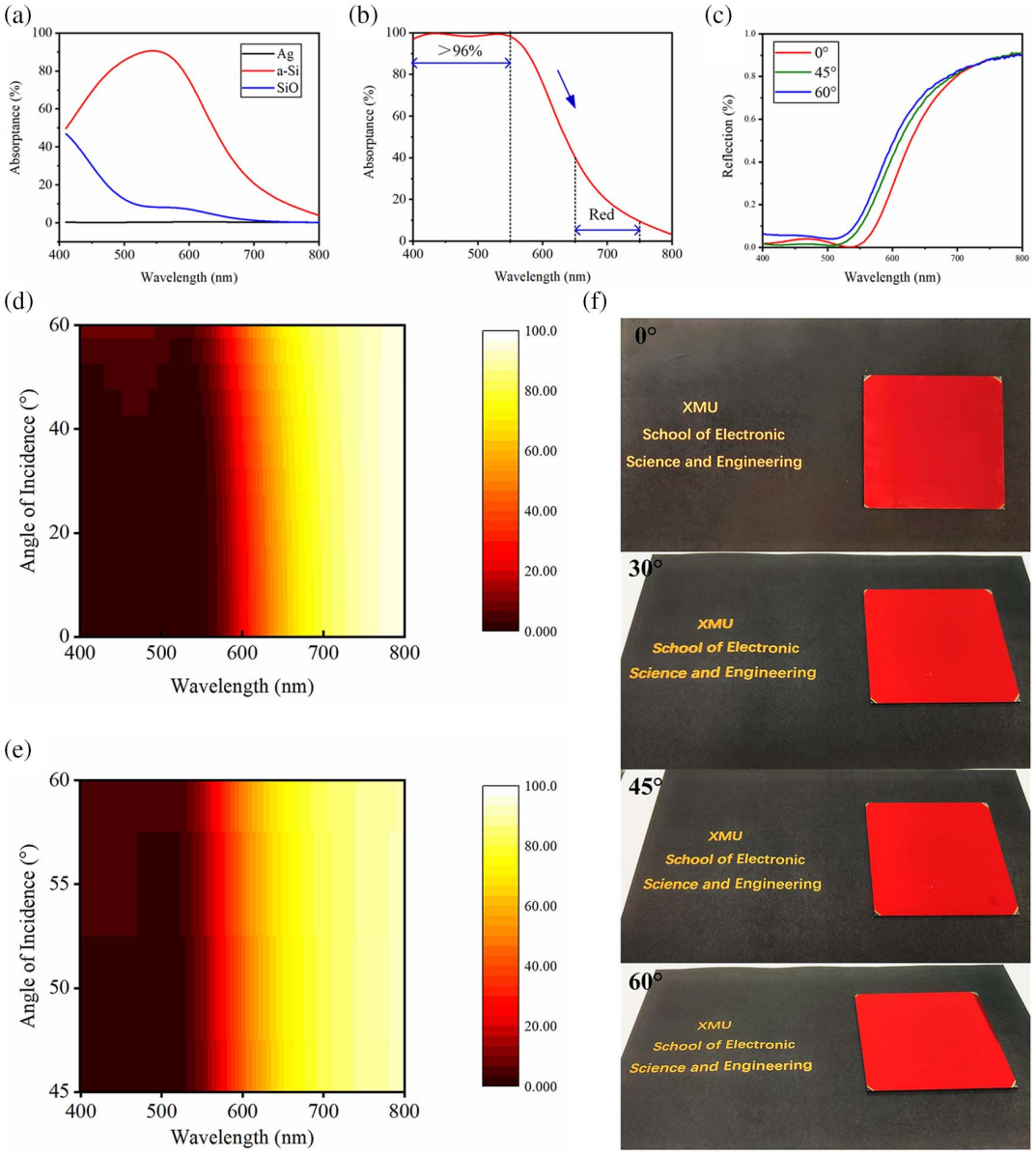

Fig. 4. (a) Absorption spectrum of Ag (black), a-Si (red), and SiO (blue). (b) Absorption spectrum of whole device. (c) Reflection spectra at different incidence angles. (d), (e) Simulated and measured angle-insensitive reflection spectrum. (f) Pictures of the sample observed from different angles.

square root of the product of the refractive index of incident medium and substrate. In the visible region, the most common glass with the refractive index of 1.52 is used. The ideal AR layer has a refractive index of 1.23, but the lowest refractive index of thin film currently available is 1.38 (MgO). For most applications, the residual reflection after using single-layer AR coating is still too high. The structure proposed by us uses the combination of SiO and SiO_2 as the double-layer AR coatings. On the premise of determining the refractive index of the two materials, the extremely low reflection can be achieved by adjusting film thickness. The performance of the double-layer AR coatings is much better than that of the single-layer AR coating.

SiO is used in the double-layer AR coatings structure. In addition to cooperating with SiO_2 as AR layers, SiO has a certain effect on improving the absorption properties of the structure. Figure 4(a) presents the absorption curve of each layer of the proposed structure, and it shows that a-Si has strong absorption properties in the 500–600 nm wavelength range, which can considerably reduce the overall reflection of the structure in this range. The color purity of the structure can be improved by reducing the reflection below 600 nm. However, the absorption properties of a-Si around 400 nm are relatively low. Therefore, we cannot conclude that the whole structure has great absorption properties in the 400–600 nm wavelength range only by taking a-Si into consideration. Also, as shown in Fig. 4(a), SiO has certain absorption properties around 400 nm. So, in the 400–500 nm wavelength range, the absorption properties of these two materials are superimposed, which can make the whole structure have higher absorption at the shorter wavelengths. Figure 4(b) is the overall absorption curve of this structure. The proposed structure has high absorption in the region of the short wavelength, but not in the long-wavelength region. The absorption properties are beneficial to further reduce the reflection of the thin-film structure in the range of 400–600 nm, but it will not reduce the reflection in the long-wavelength region to a great degree. Moreover, due to the use of high refractive index materials in the design, it is ensured that the structure has high reflection in the long-wave range, so as to achieve high-purity and high-brightness red color. At the same time, the absorption properties also make the thin-film structure have a certain degree of angle insensitivity.

Figures 4(c), 4(d), and 4(e) show the reflection spectrum of the simulated structure and the actual manufactured sample where angle and wavelength vary. It can be seen from the figure that as the angle increases, the spectral shift of the structure is small. The designed structure can maintain the red appearance in the range of 0° to 60°. The picture of the sample prepared in the laboratory is shown in the Fig. 4(f), and the proposed structure has good angle properties.

4. Conclusion

All in all, we have proposed red structural color with high color purity and high brightness based on the theory of absorption and light interference. High reflection is guaranteed by providing both steep reflections (about 91% at peak) beyond 600 nm and low absorption at the longer wavelengths. During the deposition process, the roughness of the Ag layer is reduced by controlling the deposition mode and temperature, which further enhances the reflection at the longer wavelengths. By using sufficient absorption to suppress the reflection below 600 nm and the AR layers, high color purity of the structure is ensured. The proposed structure is also angle-insensitive and can maintain the red appearance within 60°. The thin films were prepared by electron beam evaporation and combined ion-assisted deposition technology. Only the deposition is required for the device fabrication, thus providing the possibility of mass production at lower cost. The design in this paper may be useful for a variety of applications including color displays, image sensors, and so on.

Acknowledgement

This work was supported by the National Key Research and Development Program (No. 2020YFC2200400) and Xiamen Science and Technology Planning Project (No. 3502Z20183003).

References

1. K. Kumar, H. Duan, R. S. Hegde, S. C. W. Koh, J. N. Wei, and J. K. W. Yang, "Printing colour at the optical diffraction limit," Nat. Nanotechnol. **7**, 557 (2012).
2. J. P. Vigneron, J.-F. Colomer, N. Vigneron, and V. Lousse, "Natural layer-by-layer photonic structure in the squamae of *Hoplia coerulea* (Coleoptera)," Phys. Rev. E **72**, 061904 (2005).
3. J. Jang, T. Badloe, Y. Yang, T. Lee, J. Mun, and J. Rho, "Spectral modulation through the hybridization of Mie-scatterers and quasi-guided mode resonances: realizing full and gradients of structural color," ACS Nano **14**, 15317 (2020).
4. A. C. Arsenault, D. P. Puzzo, I. Manners, and G. A. Ozin, "Photonic-crystal full-colour displays," Nat. Photon. **1**, 468 (2007).
5. C. Ji, K.-T. Lee, T. Xu, J. Zhou, H. J. Park, and L. J. Guo, "Engineering light at the nanoscale: structural color filters and broadband perfect absorbers," Adv. Opt. Mater. **5**, 1700368 (2017).
6. H. Zhou, J. Xu, X. Liu, H. Zhang, D. Wang, Z. Chen, D. Zhang, and T. Fan, "Bio-inspired photonic materials: prototypes and structural effect designs for applications in solar energy manipulation," Adv. Funct. Mater. **28**, 1705309 (2018).
7. P. B. Catrysse, W. Suh, S. Fan, and M. Peeters, "One-mode model for patterned metal layers inside integrated color pixels," Opt. Lett. **29**, 974 (2004).
8. K. Chung, S. Yu, C.-J. Heo, J. W. Shim, S.-M. Yang, M. G. Han, H.-S. Lee, Y. Jin, S. Y. Lee, N. Park, and J. H. Shin, "Flexible, angle-independent, structural color reflectors inspired by morpho butterfly wings," Adv. Mater. **24**, 2375 (2012).
9. J. Hong, E. Chan, T. Chang, T.-C. Fung, B. Hong, C. Kim, J. Ma, Y. Pan, R. Van Lier, S.-G. Wang, B. Wen, and L. Zhou, "Continuous color reflective displays using interferometric absorption," Optica **2**, 589 (2015).
10. S. Yokogawa, S. P. Burgos, and H. A. Atwater, "Plasmonic color filters for CMOS image sensor applications," Nano Lett. **12**, 4349 (2012).
11. T. Teng and C. Sun, "Integrating backlight with color-filter-free panel for enhancing performance of LCD," IEEE Photon. J. **12**, 7000116 (2020).
12. Y.-T. Yoon, H.-S. Lee, S.-S. Lee, S. H. Kim, J.-D. Park, and K.-D. Lee, "Color filter incorporating a subwavelength patterned grating in poly silicon," Opt. Express **16**, 2374 (2008).
13. S. Jiang, Y. Hu, H. Wu, Y. Zhang, Y. Zhang, Y. Wang, Y. Zhang, W. Zhu, J. Li, D. Wu, and J. Chu, "Multifunctional Janus microplates arrays actuated by magnetic fields for water/light switches and bio-inspired assimilatory coloration," Adv. Mater. **31**, 1807507 (2019).

14. H. J. Park, T. Xu, J. Y. Lee, A. Ledbetter, and L. J. Guo, "Photonic color filters integrated with organic solar cells for energy harvesting," ACS Nano **5**, 7055 (2011).
15. C. Yang, W. Shen, Y. Zhang, K. Li, X. Fang, X. Zhang, and X. Liu, "Compact multilayer film structure for angle insensitive color filtering," Sci. Rep. **5**, 9285 (2015).
16. C. Yang, W. Shen, Y. Zhang, H. Peng, X. Zhang, and X. Liu, "Design and simulation of omnidirectional reflective color filters based on metal-dielectric-metal structure," Opt. Express **22**, 11384 (2014).
17. Y. Hu, H. Yuan, S. Liu, J. Ni, and J. Chu, "Chiral assemblies of laser-printed micropillars directed by asymmetrical capillary force," Adv. Mater. 2002356 (2020).
18. Y.-K. R. Wu, A. E. Hollowell, C. Zhang, and L. J. Guo, "Angle-insensitive structural colours based on metallic nanocavities and coloured pixels beyond the diffraction limit," Sci. Rep. **3**, 1194 (2013).
19. J. Chu, J. Wang, J. Wang, X. Liu, Y. Zhang, L. Shi, and J. Zi, "Structural-colored silk based on Ti-Si bilayer," Chin. Opt. Lett. **19**, 051601 (2021).
20. Z. Shao, K. Wu, and J. Chen, "All-optical inverter based on carbon nanotube-polyvinyl alcohol thin film," Chin. Opt. Lett. **18**, 060603 (2020).
21. M. A. Kats, S. J. Byrnes, R. Blanchard, M. Kolle, P. Genevet, J. Aizenberg, and F. Capasso, "Enhancement of absorption and color contrast in ultra-thin highly absorbing optical coatings," Appl. Phys. Lett. **103**, 101104 (2013).
22. A. S. Rana, M. Zubair, M. S. Anwar, M. Saleem, and M. Q. Mehmood, "Engineering the absorption spectra of thin film multilayer absorbers for enhanced color purity in CMY color filters," Opt. Mater. Express **10**, 268 (2020).
23. L. Zhao, H. Liu, Z. He, and S. Dong, "Wide-angle polarization-controllable structure color based on metamaterial resonators with polarized multiband absorption peaks," IEEE Photon. J. **10**, 2700410 (2018).
24. M. A. Kats, R. Blanchard, P. Genevet, and F. Capasso, "Nanometre optical coatings based on strong interference effects in highly absorbing media," Nat. Mater. **12**, 20 (2013).
25. C. Ji, K.-T. Lee, and L. J. Guo, "High-color-purity, angle-invariant, and bidirectional structural colors based on higher-order resonances," Opt. Lett. **44**, 86 (2019).
26. K.-T. Lee, C. Ji, D. Banerjee, and L. J. Guo, "Angular- and polarization-independent structural colors based on 1D photonic crystals," Laser Photon. Rev. **9**, 354 (2015).